Photochemical and Photophysical Reactions of fac Rhenium(I) Tricarbonyl Complexes. Effects from Binucleating Spectator Ligands on Excited and Ground State Processes

ARTICLE *in* ORGANOMETALLICS · JUNE 2001

Impact Factor: 4.13 · DOI: 10.1021/om000784p

6 AUTHORS, INCLUDING:

Juan Guerrero
University of Santiago, Chile
42 PUBLICATIONS **403** CITATIONS
SEE PROFILE

Ezequiel Wolcan
National Scientific and Technical Research C…
49 PUBLICATIONS **468** CITATIONS
SEE PROFILE

Mario R. Feliz
National University of La Plata
69 PUBLICATIONS **693** CITATIONS
SEE PROFILE

G. Ferraudi
University of Notre Dame
186 PUBLICATIONS **2,476** CITATIONS
SEE PROFILE

Photochemical and Photophysical Reactions of *fac*-Rhenium(I) Tricarbonyl Complexes. Effects from Binucleating Spectator Ligands on Excited and Ground State Processes

J. Guerrero,[§] O. E. Piro,[⊥] E. Wolcan,[†] M. R. Feliz,*[,†] G. Ferraudi,*[,‡] and S. A. Moya*[,§]

INIFTA(CONICET), Universidad Nacional de La Plata, C.C. 16, Suc. 4, 1900 La Plata, Argentina, Radiation Laboratory, University of Notre Dame, Notre Dame, Indiana 46556-0579, Department of Applied Chemistry, Facultad de Química y Biología, Universidad de Santiago, Casilla 40, Correo 33, Santiago, Chile, and Department of Physics, Facultad de Ciencias Exactas, Universidad Nacional de La Plata and PROFIMO(CONICET), C.C. 67, 1900 La Plata, Argentina

Received September 13, 2000

Ground and excited state properties of the newly prepared complexes $Re(CO)_3$(2,2′-biquinoline)L_S^+, L_S = pyrazine or 4,4′-bipyridine, and $Re(CO)_3$(2,2′-bipy)(2-pyrazinecarboxylate) were investigated by steady state and time-resolved spectroscopy. The X-ray structure of the latter compound showed that the spectator ligand 2-pyrazinecarboxylate is coordinated through the carboxylate group to Re(I). A component of the complexes' luminescence was associated with long-lived Re to ligand, 2,2′-biquinoline or 2,2′-bipy, charge transfer, while a fast component of the emission was associated with intraligand excited states. Quenching of the luminescence by $CuCl_2$ involved energy transfer via dynamic and static mechanisms. The complexes in their excited states were reduced by 2,2′,2″-nitrilotriethanol with the formation of Re(I) ligand-radical species. Similar products were generated by the pulse radiolytic reduction of the complexes. The photochemical properties of the 2,2′-biquinoline complexes and $Re(CO)_3$(1,10-phen)4-nitrobenzoate are compared, and the mechanisms of their photochemical reactions are discussed.

Introduction

The substitution of a halide X by the spectator ligand L_S in $Re^I(CO)L_AX$, where L_A is a bis monodentated azine or a bidentate azine, has provided useful procedures for the preparation of related $Re^I(CO)_3L_AL_S$ complexes.[1−7] In homologous series of these complexes, the constituents have a common chromophore, $-Re^I(CO)L_A$, and the spectator ligand L_S is varied in a judicious manner through the series. The series of compounds provided experimental bases for the investigation of the $-Re^I(CO)L_A$ photophysics as a function of the L_S ligand.[6] Literature reports show, for example, that the function of L_S is to exert small perturbations that alter the electronic structure of the chromophore and modify its photophysics.[6]

Interactions of L_S with the chromophore can be sufficiently strong and the spectator ligand can be engaged in redox processes together with L_A. Indeed, competitive electron transfer to L_A and L_S was observed in the ground and excited states of $Re(CO)_3$(4-nitrobenzoate)L_A, L_A = 1,10-phenanthroline, 2,2′-bipyridine, and (4-phenylpyridine)$_2$. The reduction of the complexes by $^\bullet CH_2OH$ radicals is followed by an equilibration between species of Re(I) with coordinated ligand-radicals, eqs 1, 2.[7]

$$Re(CO)_3(4\text{-}O_2CC_6H_4NO_2)L_A + {}^\bullet CH_2OH \rightarrow Re(CO)_3(4\text{-}O_2CC_6H_4NO_2^\bullet)L_A^- + CH_2O + H^+ \quad (1)$$

$$Re(CO)_3(4\text{-}O_2CC_6H_4NO_2^\bullet)L_A^- \rightleftharpoons Re(CO)_3(4\text{-}O_2CC_6H_4NO_2)(L_A^\bullet)^- \quad (2)$$

By contrast to the ground state reactions, a Re(I) to 4-nitrobenzoate, NO_2Bz, charge-transfer excited state, $MLCT_{NO_2Bz\leftarrow Re}$, is produced by a complex photochemical

* To whom correspondence should be addressed.
† INIFTA(CONICET), Universidad Nacional de La Plata.
‡ University of Notre Dame.
§ Universidad de Santiago.
⊥ Universidad Nacional de La Plata and PROFIMO(CONICET).

(1) Abbreviations used in this work: 2,2′,2″-nitrilotriethanol, TEOA; 4-nitrobenzoate, NO_2Bz; pyrazine, pz; 2-carboxylate-1,4-diazine, pz-CO_2; 2,2′-biquinoline, (2,2′-biq); metal-to-ligand charge-transfer excited state, MLCT; intraligand excited state, IL.

(2) Moya, S. A.; Guerrero, J.; Pastene, R.; Schmidt, R.; Sariego, R.; Sartori, R.; Sanzaparicio, J.; Fonseca, I.; Martinezripoll, M. *Inorg. Chem.* **1994**, *33*, 2341.
(3) Guerrero, J.; Moya, S. A., Garland, M. T.; Baggio, R. F. *Acta Crystallogr. Sect. C* **1999**, *55*, 932.
(4) Bates, W. D.; Chem, P. Y.; Jones, W. E.; Meyer, T. J. *J. Phys. Chem.* **1999**, *103*, 5227.
(5) Ferraudi, G.; Feliz, M. R.; Wolcan, E.; Hsu, I.; Moya, S. A.; Guerrero, J. *J. Phys. Chem.* **1995**, *99*, 4929.
(6) Sacksteder, L.; Zipp, A. P.; Brown, E. A.; Streich, J.; Demas, J. N.; DeGraff, B. A. *Inorg. Chem.* **1990**, *29*, 4335.
(7) Ferraudi, G.; Feliz, M. R. *Inorg. Chem.* **1998**, *37*, 2806.

10.1021/om000784p CCC: $20.00
Publication on Web 05/22/2001

mechanism, eqs 3−5. Photogeneration of a Re to the azine ligand charge-transfer excited state, $MLCT_{Azine\leftarrow Re}$ and its equilibration with an intraligand excited state, IL, precede the formation of the MLCT $_{NO_2Bz\leftarrow Re}$, eqs 3−5.

$$Re(CO)_3(4\text{-}O_2NC_6H_4CO_2)azine + h\nu \rightarrow MLCT_{Azine\leftarrow Re} \quad (3)$$

$$MLCT_{Azine\leftarrow Re} \rightleftharpoons IL \quad (4)$$

$$IL \rightarrow MLCT_{NO_2Bz\leftarrow Re} \quad (5)$$

Additional interest in the properties that L_S imposes on $-Re^I(CO)_3L_A$ is brought about by possible applications to biochemical processes[8−11] and to the CO_2 reduction.[12] Also the derivatization of polymers with chromophores, e.g., $-Re^I(CO)_3L_A$,[3] has prompted an investigation of the role of L_S in the reactivity of some Re(I) monomers. In this work, we have studied the photophysics and redox reactivity of Re(I) complexes, $Re^I(CO)_3L_AL_S$, with L_A = 2,2′-bipyridine (2,2′-bipy), 2,2′-biquinoline ((2,2′-biq) shown in (I)), and binucleating ligands L_S = pyrazine (pz shown in (II)), 4,4′-bipyridine (4,4′-bipy shown in (III)), and 2-pyrazinecarboxylate (pz-CO_2). In the structures (II) and (III), dashed lines indicate the atom used for the coordination to Re.

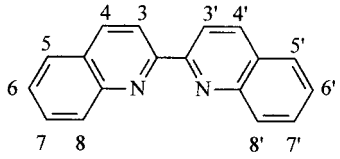

(I) 2,2'-biq = 2,2'-biquinoline

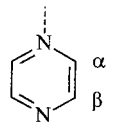

(II) pz = pyrazine

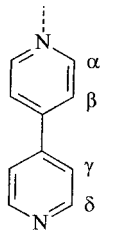

(III) 4,4'-bipy = 4,4'-bipyridine

Experimental Section

Flash-Photochemical Procedures. Optical density changes occurring on a time scale longer than 10 ns were investigated with a flash photolysis apparatus, FP, and procedures described elsewhere.[14,15] In these experiments, 10 ns flashes of 351 nm light were generated with a Lambda Physik SLL-200 excimer laser, or 1 ns flashes of 355 nm light were generated with a Continuum Powerlite Nd:YAG laser.[14,15] The energy of the laser flash was attenuated to values equal to or less than 20 mJ/pulse by absorbing some of the laser light in solutions of $Ni(ClO_4)_2$ with appropriate optical densities. Time-resolved fluorescence experiments, FF, were carried out with a PTI flash fluorescence instrument. The excitation light was provided by a N_2 laser with a 0.2 ns pulse width and ca. 2 mJ/pulse. Solutions for the photochemical work were deaerated with streams of ultrahigh-purity N_2 before and during the irradiations. Concentrations of the complexes were adjusted to provide homogeneous concentrations of photogenerated intermediates within the volume of irradiated solution, i.e., optical densities less than or equal to 0.1 at λ_{exc} nm in a 1 cm optical path.

Pulse-Radiolytic Procedures. Optical pulse radiolysis measurements were carried out with a system and procedures similar to those described earlier.[16,17] In this procedure, the dose/pulse was evaluated by means of the $(SCN)_2^-$ radical concentrations produced in the radiolysis cell by the electron pulse. The average concentrations of $(SCN)_2^-$ radical used in the experiments were $(2.0 \pm 0.2) \times 10^{-5}$ or $(1.0 \pm 0.1) \times 10^{-5}$ M. A flow system was used to ensure that fresh solution was brought to the reaction cell between electron pulses. Solutions for the irradiation were prepared by adding the solid compounds to liquids previously deaerated with streams of O_2-free gases, i.e., N_2O and N_2. Radiolysis with ionizing radiation of CH_3OH and CH_3OH/H_2O mixtures has been reported elsewhere in the literature.[18,19] These studies have shown that pulse radiolysis can be used as a convenient source of e^-_{solv} and $^\bullet CH_2OH^\bullet$ radicals according to eq 6. Since e^-_{solv}

$$\begin{array}{ccccc} CH_3O^\bullet + H^+ & & & & \cdot CH_2OH + CH_3OH \\ \uparrow & & & & \uparrow + CH_3OH \\ \rightarrow \quad CH_3OH^+ & + & e^-_{solv} & + & CH_3O^\bullet + H^+ \\ & & & & \downarrow + CH_3OH + N_2O \\ & & & & \cdot CH_2OH + N_2 + OH^- \end{array} \quad (6)$$

and $^\bullet CH_2OH$ have large reduction potentials, i.e., −2.8 V vs NHE for e^-_{solv} and −0.92 V vs NHE for $^\bullet CH_2OH$, they can be used for the reduction of coordination complexes and for the study of electron-transfer reactions. The yield of e^-_{solv} in CH_3OH ($G \approx 1.1$) is about a third of the G-value in the radiolysis of H_2O ($G \approx 2.8$).[18,19] In solutions where e^-_{solv} was scavenged with N_2O, the $^\bullet CH_2OH^\bullet$ radical appears to be the predominant product (yield > 90%) of the reaction between CH_3OH and O^-.

Steady-State Irradiations. The luminescence of the Re(I) complexes was investigated in an SLM-Aminco-8100 interfaced to a Dell 333P microcomputer.[6] The spectra was corrected for differences in instrumental response and light scattering. Solutions were deaerated with O_2-free nitrogen in a gastight apparatus before recording the spectra.

(8) West, F.; Scotian, M. B.; Leibnitz, P.; Spies, H.; Katzenellenbogen, J. A.; Johannsen, B. *Bioorg. Med. Chem.* **1999**, *7*, 1827.
(9) Yam, V. W. W.; Lo, K. K. W.; Cheung, K. K.; Kong, R. Y. C. *J. Chem. Soc., Dalton Trans.* **1997**, 2067.
(10) Guo, X. Q.; Castellano, F. N.; Li, L.; Szmacinski, H.; Lackowicz, J. R.; Spoor, J. *Anal. Biochem.* **1997**, *254*, 179.
(11) Terpetschnig, E.; Szmacinski, H.; Lackowicz, J. R. *Fluoresc. Spectrosc.* **1997**, *278*, 295.
(12) Hori, H.; Ishihara, J.; Koike, K.; Takeuchi, K.; Ibusuki, T.; Ishitani, O. *J. Photochem. Photobiol. A-Chem.* **1999**, *120*, 119.
(13) Wolcan, E.; Ferraudi, G. *J. Phys. Chem. A* **2000**, *104*, 9281.
(14) Sarakha, M.; Ferraudi, G. *Inorg. Chem.* **1999**, *38*, 4605.
(15) Sarakha, M.; Cozzi, M.; Ferraudi, G. *Inorg. Chem.* **1996**, *35*, 3804.
(16) (a) Hugh, G. L.; Wang, Y.; Schöneich, C.; Jiang, P.-Y.; Fesenden, R. W. Radiat. *Phys. Chem.* **1999**, 54, 559. (b)Vargas, J.; Ferraudi, G.; Canale, J.; Costamagna, J. *Inorg. Chim. Acta* **1994**, *226*, 151.
(17) Buxton, G. V.; Greenstock, C. L.; Hellman, W. P.; Ross, A. B. *J. Phys. Chem. Ref. Data* **1988**, *17*, 513.
(18) Getoff, N.; Ritter, A. *Schworer Radiat. Phys. Chem.* **1993**, *41*, 797.
(19) Dorfman, L. M. In *The Solvated Electron in Organic Liquids*; Gould, R. F., Ed.; Advanced Chemistry Series; American Chemical Society: Washington, DC, 1965.

Electrochemical Procedures. Electrochemical measurements were carried out with a PAR 173 potentiostat coupled to a PAR 175 universal programmer. Deaerated solutions, 10^{-4} M complex and 10^{-2} M tetraethylammonium perchlorate in a given solvent, were placed in a three-electrode cell with a glassy carbon working electrode, a Pt wire counter electrode, and a saturated calomel reference electrode. Solvents and supporting electrolyte for the electrochemical measurements were dried according to literature procedures.[20,21]

Materials. Re(CO)$_3$(2,2′-bipy)O$_2$C-pz was prepared by a modification of a literature procedure.[1−6,22,23] Solid Ag(CF_3SO_3) and the sodium salt of pz-CO_2^- were added in succession to a warm solution of Re(CO)$_3$(2,2′-bipy)Br (2 or 5 g) in CH_3CN (100 cm^3). The reactants were respectively in a 1:1 stoichiometry and in a 10% excess from a 1:1 stoichiometry in relationship to the Re(I). The reacting mixture was stirred overnight while kept in the dark and at room temperature. The Re(I) complex in the CH_3CN solution was precipitated by adding pentane after removal of the other product, solid AgBr, by filtration. The raw material was purified by column chromathography on alumina. The complex was easily eluted, by comparison to other species, with MeOH/$CHCl_3$ mixtures. A pure material was collected by rotoevaporation of several chromatographic fractions. Anal. Calcd for $ReC_{18}H_{11}N_4O_5$: H, 2.02; C, 39.34; N, 10.20. Found: H, 2.00; C, 38.70; N, 9.80.

Re(CO)$_3$(2,2′-biq)OSO$_2$CF$_3$ was obtained by treating a solution of Re(CO)$_3$(2,2′-biq)Br in methylene chloride with a stoichiometric amount of silver triflate at 50 °C under dry N_2. A precipitate of silver bromide was filtered off through Celite. The product was purified by column chromatography on alumina with methylene chloride as eluent, and the fractions with the eluted Re(I) complex were concentrated by rotoevaporation. Pure crystals were isolated by recrystallization from methylene chloride. Anal. Calcd for $ReC_{22}H_{12}N_2O_6SF_3$: H, 1.79; C, 39.11; N, 4.15. Found: H, 2.01; C, 39.71; N, 4.32

[Re(CO)$_3$(2,2′-biq)pz]CF$_3$SO$_3$. A solution of Re(CO)$_3$(2,2′-biq)OSO$_2$CF$_3$ in methylene chloride was stirred at 50 °C with a stoichiometric amount of pz. The resulting orange solution was concentrated and the product purified by column chromatography on alumina. The starting material was eluted with methylene chloride, and the complexes were eluted with a solution of 5% v/v methanol in methylene chloride. The solution was concentrated, and a microcrystalline orange product was obtained after dropwise addition of chilled hexane. The product was filtered, washed with a cool methylene chloride/hexane mixture, and dried under vacuum. Anal. Calcd for $ReC_{26}H_{16}N_4O_6SF_3$: H, 2.13; C, 41.32; N, 7.41. Found: H, 1.89; C, 42.02; N, 7.05.

[Re(CO)$_3$(2,2′-biq)4,4′-bipy]CF$_3$SO$_3$ was obtained by the same procedure used for the preparation of [Re(CO)$_3$(2,2′-biq)-pz]CF_3SO_3 with the exception of the use of 4,4′-bipyridine instead of pz. Anal. Calcd for $ReC_{32}H_{20}N_4O_6SF_3$: H, 2.42; C, 46.21; N, 6.74. Found: H, 2.20; C, 47.01; N, 6.74.

The starting materials 2,2′-biq, Re(CO)$_3$(2,2′-bipy)Br, and Re(CO)$_3$(2,2′-biq)Br were available from previous works.[2,5,7] Other materials were reagent grade and used without further purification.

Determination of the Crystal Structure. Crystals of Re(CO)$_3$(2,2′-bipy)O$_2$C-pz were grown by slow evaporation of the solvent from a concentrated solution of the complex in CH_3CN. The yellow-green/plate crystal used for X-ray crystallography had the approximate dimensions of 0.06 × 0.24 × 0.24 mm and was mounted on a glass fiber in a random orientation. Crystallographic parameters are shown in Table 1.

Diffraction Data and Structure Solution and Refinement. Crystal data, data collection procedure, structure determination methods, and refinement results are summarized in Table 1.[24−29] The samples were very thin crystal plates that diffracted poorly. Only about 64% of the X-ray intensity data up to 0.76 Å resolution were above two standard deviations of measurement errors.

Table 1. Crystal Data, Structure Solution Methods, and Refinement Results for Re(CO)$_3$(2,2′-bipy)O$_2$C-pz

empirical formula	$C_{18}H_{11}N_4O_5Re$
fw	549.51
temperature	293(2) K
cryst system	monoclinic
space group	$P2_1/a$
unit cell dimens[a]	$a = 9.168(3)$ Å $b = 10.896(2)$ Å $c = 17.551(3)$ Å $\beta = 96.21(2)°$
volume	1743.0(6) Å^3
Z	4
density (calcd)	2.094 Mg/m^3
abs coeff	7.012 mm^{-1}
$F(000)$	1048
cryst size	0.06 × 0.24 × 0.24 mm
crystal color/shape	yellow-green/plate
diffractometer/scan	Enraf-Nonius CAD-4/ω-2θ
radiation, graphite monochromator	Mo Kα, $\lambda = 0.71073$ Å
scan width	$0.8 + 0.35 \tan\theta$
standard refln	(5, 4, −8)
decay of standard	±2.9
θ range for data collection	1.17−27.95°
index ranges	$-12 \le h \le 11$, $0 \le k \le 14$, $0 \le l \le 23$
no. of reflns collected	4679
no. of ind reflns	3722 [R(int) = 0.033]
no. of obsd reflns [$I > 2\sigma(I)$]	2872
data reduction and correction[b] and structure solution[c] and refinement[d] programs	SDP,[22] SHELX-76,[23] SHELF-86,[24] SHELF-93,[25]
refinement method	full-matrix least-squares on F
weights, w	$w = [\sigma^2(F_o^2) + (0.107P)^2]^{-1}$, $P = [\mathrm{Max}(F_o^2,0) + 2F_c^2]/3$
no. of data/restraints/params	3722/0/254
goodness-of-fit on F^2	1.073
final R indices [$I > 2\sigma(I)$]	R1 = 0.050, wR2 = 0.129
R indices (all data)	R1 = 0.072, wR2 = 0.153
largest diff peak and hole	3.5[f] and −2.94 e Å^{-3}

[a] Least-squares refinement of [(sin θ)/λ]^2 values for 25 reflections in the 24.8° < 2θ < 36.9° range. [b] Corrections: Lorentz, polarization, and absorption.[21] Maximum and minimum transmission factors of 0.671 and 0.220. [c] Neutral scattering factors and anomalous dispersion corrections. [d] Structure solved by Patterson and Fourier methods and the final molecular model obtained by anisotropic full-matrix least-squares refinement of non-hydrogen atoms. [e] R indices defined as: $R1 = \sum||F_o| - |F_c||/\sum|F_o|$, $wR2 = [\sum w(F_o^2 - F_c^2)^2/\sum w(F_o^2)^2]^{1/2}$. [f] Close to the rhenium atom position.

Several H atoms were detected at approximate locations in a difference Fourier map. They were stereochemically positioned and refined with the riding model by utilizing a common isotropic displacement parameter. Such a parameter converged to $U = 0.06(1)$ Å^2. Bond distances and angles are in Table 2. Additional crystallographic data are provided in the Supporting Information.

(20) Coetzee, J. F.; Cunningham, g. P.; McGuire, D. K.; Padmanabhan, G. R. *Anal. Chem.* **1962**, *31*, 1139.
(21) Kolhoff, I. M.; Coetzee, J. F. *J. Am. Chem. Soc.* **1957**, *79*, 870.
(22) Zingales, F.; Satorelli, L.; Trovati, A. *Inorg. Chem.* **1967**, *6*, 1246.
(23) Zingales, F.; Graziani, M.; Faraone, F.; Belluco, U. *Inorg. Chim. Acta* **1967**, *1*, 172.
(24) Busing, W. R.; Levy, H. A. *Acta Crystallogr.* **1957**, *10*, 180.
(25) Frenz, B. A. *Enraf-Nonius Structure Determination Package*; Enraf-Nonius: Delft, The Netherlands, 1983.
(26) Sheldrick, G. M. *SHELX, a Program for Crystal Structure Determination*; University of Cambridge: Cambridge, England, 1976.
(27) Sheldrick, G. M. *Acta Crystallogr.* **1990**, *A46*, 467.
(28) Sheldrick, G. M. *SHELXL93, a Program for Crystal Structure Refinement*; University of Göttingen: Germany, 1993.
(29) Johnson, C. K. *ORTEP*, Report ORNL-3794; Oak Ridge, TN, 1965.

Table 2. Bond Distances (Å) and Angles (deg) for *fac*-Re(CO)$_3$(2,2′-bipy)O$_2$C-pz[a]

Bond Distances	
Re−C(1)	1.883(11)
Re−C(3)	1.904(12)
Re−C(2)	1.909(11)
Re−N(22)	2.162(8)
Re−N(21)	2.164(8)
Re−O(11)	2.205(7)
C(1)−O(1)	1.195(13)
C(2)−O(2)	1.148(13)
C(3)−O(3)	1.117(14)
O(11)−C(4)	1.238(13)
O(12)−C(4)	1.208(13)
C(4)−C(11)	1.499(14)
C(11)−N(11)	1.330(11)
C(11)−C(14)	1.389(14)
N(11)−C(12)	1.35(2)
C(12)−C(13)	1.34(2)
C(13)−N(12)	1.34(2)
N(12)−C(14)	1.34(2)
N(21)−C(21)	1.320(14)
N(21)−C(25)	1.399(13)
C(21)−C(22)	1.381(13)
C(22)−C(23)	1.35(2)
C(23)−C(24)	1.38(2)
C(24)−C(25)	1.371(13)
C(25)−C(26)	1.456(14)
C(26)−N(22)	1.355(10)
C(26)−C(27)	1.40(2)
C(27)−C(28)	1.37(2)
C(28)−C(29)	1.38(2)
C(29)−C(210)	1.39(2)
C(210)−N(22)	1.318(14)
Bond Angles	
C(1)−Re−C(3)	87.8(4)
C(1)−Re−C(2)	87.7(5)
C(3)−Re−C(2)	89.5(5)
C(1)−Re−N(22)	99.9(4)
C(3)−Re−N(22)	93.0(4)
C(2)−Re−N(22)	172.0(4)
C(1)−Re−N(21)	175.1(4)
C(3)−Re−N(21)	93.7(4)
C(2)−Re−N(21)	96.9(4)
N(22)−Re−N(21)	75.5(3)
C(1)−Re−O(11)	94.9(4)
C(3)−Re−O(11)	174.0(4)
C(2)−Re−O(11)	95.9(4)
N(22)−Re−O(11)	81.3(3)
N(21)−Re−O(11)	83.1(3)
O(1)−C(1)−Re	175.0(9)
O(2)−C(2)−Re	177.7(10)
O(3)−C(3)−Re	179.9(8)
C(4)−O(11)−Re	121.2(6)
O(12)−C(4)−O(11)	127.1(10)
O(12)−C(4)−C(11)	116.6(10)
O(11)−C(4)−C(11)	116.1(9)
N(11)−C(11)−C(14)	121.5(10)
N(11)−C(11)−C(4)	119.6(9)
C(14)−C(11)−C(4)	118.9(10)
C(11)−N(11)−C(12)	115.7(10)
C(13)−C(12)−N(11)	122.3(12)
N(12)−C(13)−C(12)	123.2(12)
C(13)−N(12)−C(14)	115.1(10)
N(12)−C(14)−C(11)	122.0(11)
C(21)−N(21)−C(25)	117.2(9)
C(21)−N(21)−Re	125.8(7)
C(25)−N(21)−Re	116.9(6)
N(21)−C(21)−C(22)	123.2(11)
C(23)−C(22)−C(21)	119.6(11)
C(22)−C(23)−C(24)	119.4(10)
C(25)−C(24)−C(23)	119.5(11)
C(24)−C(25)−N(21)	121.0(10)
C(24)−C(25)−C(26)	125.6(9)
N(21)−C(25)−C(26)	113.4(8)
N(22)−C(26)−C(27)	120.3(10)
N(22)−C(26)−C(25)	117.7(8)
C(27)−C(26)−C(25)	121.9(8)
C(28)−C(27)−C(26)	119.6(10)
C(27)−C(28)−C(29)	119.7(11)
C(28)−C(29)−C(210)	117.3(12)
N(22)−C(210)−C(29)	124.2(11)
C(210)−N(22)−C(26)	118.8(9)
C(210)−N(22)−Re	125.0(7)
C(26)−N(22)−Re	116.2(7)

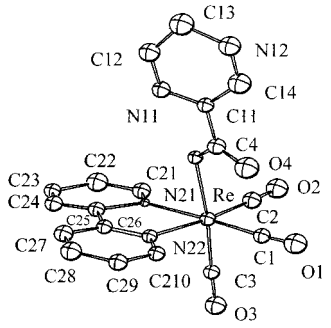

Figure 1. ORTEP drawing of Re(CO)$_3$(2,2′-bipy)O$_2$C-pz showing the labeling of the non-H atoms and their vibrational ellipsoids at 30% probability.[26]

Results

Characterization of the Re(I) Complexes. The IR and NMR spectra of the Re(CO)$_3$(2,2′-biq)L$_S^+$, L$_2$ = pz or 4,4′-bipy, in Table 3 showed that they are structurally related to previously prepared Re(I) compounds of the 2,2′-biq ligand.[1,2] The crystallographic structure of Re(CO)$_3$(2,2′-bipy)O$_2$C-pz has demonstrated that pz-CO$_2^-$ coordinated to Re by its carboxylate group, Figure 1.[29] No linkage isomers of the Re(CO)$_3$(2,2′-bipy)O$_2$C-pz were produced during the preparation or thereafter. The rhenium atom is in a distorted octahedral environment. It is coordinated by two carbonyl groups [mean Re−C distance of 1.90(1) Å] and a 2,2′-bipyridyl molecule acting as a bidentate ligand [mean Re−N distance of 2.163(8) Å], which define an equatorial plane. The octahedral coordination is completed at the axial positions by another CO ligand [d(Re−C) = 1.90(1) Å] and a carboxyl oxygen of a pyrazine molecule [d(Re−O) = 2.205(7) Å]. As expected, the 2,2′-bipyridyl and pyrazine rings and the carboxylate C−CO$_2$ group are planar to within experimental accuracy. The two 2,2′-bipyridyl rings are slightly tilted [in 8.2(6)°] from each other. The C−CO$_2$ plane is tilted in 28.0(6)° from the pyrazine ring. Both planes depart from perpendicularity with the best least-squares plane through the 2,2′-bipyridyl ligand by about 12°. The Re atom lies approximately on the intersection of the equatorial plane defined by this ligand and the carboxyl plane.

Redox Properties. Deaerated solutions in CH$_3$CN with concentrations close to 10^{-3} M of a given Re(I) complex and 10^{-1} M tetrabutylamonium hexafluorophosphate as supporting electrolyte were used for cyclic voltammetry. Scan rates between 250 and 2000 mV/min were used for these experiments. The voltammograms for Re(CO)$_3$(2,2′-bipy)O$_2$C-pz and Re(CO)$_3$(2,2′-bipy)Br exhibited similar features, i.e., reversible waves at 1.32 vs SCE corresponding to the Re(II/I) couple and −1.33 vs SCE assigned to the coordinated 2,2′-bipy/2,2′-bipy$^{\bullet-}$, Table 4.[30] Additional waves were observed at more negative potentials, and they were assigned to the reduction of the spectator ligand pz-CO$_2^-$.

Absorption Spectra. The UV−vis spectra of the Re(I) complexes exhibited absorption bands similar to those observed in the spectra of related Re(I) complexes with L$_S$ = Br, Figure 2. No spectral features corre-

(30) Values extracted from: Meites, L.; Zuman, P. In *Handbook Series in Organic Electrochemistry*; CRS Press: Cleveland, 1976; Vols. I, II.

Table 3. IR Carbonyl Frequencies and NMR Resonances in $Re(CO)_3(2,2'\text{-biq})L^+$ Complexes

ligands		ν_{CO} cm^{-1}	^{1}H NMR assignments[a]					
			$Re(CO)_3(2,2'\text{-biq})OSOCF_3$					
OSO_2CF_3	2,2′-biq	2029	$H_{3,3'}$	$H_{4,4'}$	$H_{5,5'}$	$H_{6,6'}$	$H_{7,7'}$	$H_{8,8'}$
		1935	8.41d	8.67s	8.03m	7.83t	8.03m	8.92d
		1914						
			$Re(CO)_3(2,2'\text{-biq})pz^+$					
	2,2′-biq	2030	$H_{3,3'}$	$H_{4,4'}$	$H_{5,5'}$	$H_{6,6'}$	$H_{7,7'}$	$H_{8,8'}$
		1930	8.86d	8.91d	8.16dd	7.93st[b]	8.12st[b]	8.82dd
		1915						
pz			H_α	H_β				
			7.35d	8.48d				
			$Re(CO)_3(2,2'\text{-biq})(4,4'\text{-bipy})^+$					
	2,2′-biq	2032	$H_{3,3'}$	$H_{4,4'}$	$H_{5,5'}$	$H_{6,6'}$	$H_{7,7'}$	$H_{8,8'}$
		1914	8.82d	8.88d	8.14d	7.90st[b]	8.12st[b]	8.83dd
4,4′-bipy			H_α	H_β	H_γ	H_δ		
			7.30d	7.26d	7.51d	8.72d		

[a] Protons defined in structures (I)−(III) elsewhere in this work. Shifts are in ppm from TMS, $CDCl_3$-d_1. [b] Pseudotriplet.

Table 4. Electrochemical Properties of Re(I) Complexes and Related Ligands

	$E_{1/2}$, V[a]			
	+3e	+2e	+1e	−1e
$Re(CO)_3(2,2'\text{-biq})pz^+$	−1.22[b]	−0.88	−0.73	+1.46
$Re(CO)_3(2,2'\text{-biq})4,4'\text{-bipy}^+$	−1.23[b]	−0.91	- 0.74	+1.2[c]
$Re(CO)_3(2,2'\text{-bipy})O_2C\text{-pz}$	−2.2[c]	−1.9[b]	−1.33[b]	+1.33[b]
(2,2′-biq)			−0.94[1]	
4,4′-bipy[d]			−0.73[27]	
pz			$-0.25 \geq E^0 \geq -0.885$ [e,27]	
2,2′-bipy[d]			−0.74[27]	

[a] Half-wave potentials relative to the SCE recorded with a scan rate of 2000 mV/s. The potentials did not experience changes when the scan rate was reduced to 250 mV/s. [b] Reversible or quasi reversible processes. [c] Peak potentials without counterwave. [d] Diprotonated cation. The reduction of the monoprotonated cation is estimated to be displaced between −0.5 and −1.0 V from the diprotonated cation. [e] Potentials reported in aqueous solutions for various acid concentrations, $0 \leq pH \leq 6.8$.

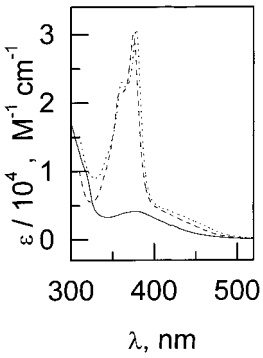

Figure 2. Absorption spectra of Re(I) complexes: $Re(CO)_3(2,2'\text{-biq})pz^+$ (– – –), $Re(CO)_3(2,2'\text{-biq})(4,4'\text{-bipy})^+$ (•••), and $Re(CO)_3(2,2'\text{-bipy})O_2C\text{-pz}$ (—) in MeOH.

sponding to ligand-to-ligand and/or Re-to-spectator ligand charge-transfer transitions could be discerned. In the case of the $Re(CO)_3(2,2'\text{-biq})L_S^+$, L_S = pz or 4,4′-bipy, the redox potentials, Table 4, show that Re(I) to L_S charge-transfer transitions must be placed at lower energies than the Re(I) to 2,2′-biq transitions. Intraligand transitions localized in the (2,2′-biq) at $\lambda_{max} \approx$ 375 nm are prominent in the spectra of the $Re(CO)_3(2,2'\text{-biq})L_S^+$ complexes, Figure 2.

Steady-State Luminescence. In the absorption spectrum of the Re(I) complexes, the first absorption band can be assigned to a Re(I) to L_A charge-transfer transition, Figure 2. By contrast, the more intense absorptions at 350 nm or shorter wavelengths correspond to an overlap of the charge-transfer transition and an intraligand transition. Irradiation of the complexes at such wavelengths, λ_{exc}, provided abundant information about the photophysical processes. The emission spectrum of $Re(CO)_3(2,2'\text{-bipy})O_2C\text{-pz}$ changed with solvent and excitation wavelength, Figure 3a. The broad emission band recorded in deaerated CH_3CN is appreciably narrowed and acquires a more symmetric

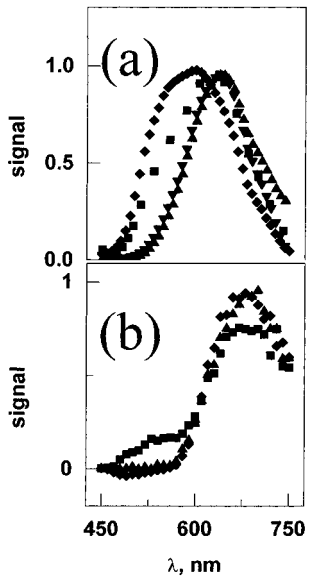

Figure 3. Emission spectra of Re(I) complexes. The spectrum of $Re(CO)_3(2,2'\text{-bipy})O_2C\text{-pz}$ (a) was recorded with N_2-deaerated solutions of the complex in CH_3CN (♦♦♦, λ_{exc} = 350 nm and ▲▲▲, λ_{exc} = 400 nm) or CH_2Cl_2 (▼▼▼, λ_{exc} = 350 nm and ■■■, λ_{exc} = 400 nm). The spectrum of $Re(CO)_3(2,2'\text{-biq})(4,4'\text{-bipy})^+$ (b) was recorded in N_2-deaerated CH_3CN (■■■, λ_{exc} = 350 nm and ▲▲▲, λ_{exc} = 400 nm) or CH_2Cl_2 (♦♦♦, λ_{exc} = 400 nm).

Table 5. Excited State Lifetimes of $Re(CO)_3L_AL_S$ Complexes

L_A	L_S	τ_1, ns	τ_2, ns	A_1/A_2[a]	conditions[b]
(2,2′-biq)	pz	4.1	113	2.0	S_1, FF
		6	114	1.5	S_2, FF
			80		S_2, FP
	4,4′-bipy	5	58	1.3	S_1, FF
			65		S_1, FP
			63		S_2, FP
	py		57		S_1, FP
	Br		5		S_2, FF
	CH_3CN		76		S_2, FP
2,2′-bipy	pz-CO_2	26	518	2.5	S_2, FP
		22	405	0.7	S_2, FF
		23	109	0.5	S_3, FF
	Br		99		S_3, FF

[a] Relative preexponential factors for the biexponential decay of the luminescence. [b] Lifetimes measured in deaerated S_1 = 4% v/v CH_3OH in CH_2Cl_2; S_2 = CH_3CN; S_3 = CH_2Cl_2 with 355 and/or 351 nm laser flash photolysis, FP, or 337 nm laser flash fluorescence, FF, techniques. The kinetics of the luminescence was investigated at the wavelength of the maximum in the emission spectrum. Each lifetime from FP experiments is an average of traces recorded at different wavelengths.

shape when the excitation is changed from 350 to 400 nm. In deaerated CH_2Cl_2 the change of λ_{exc} = 350 nm to 400 nm produces a displacement of the emission that has the reverse sense of that observed in CH_3CN. The spectral shifts with solvent and the wavelength of excitation indicated that there are at least two contributions to the envelop of the emission band. One contribution to the emission, centered at 650 nm, appears to be the less affected by changes of λ_{exc} or solvent. The steady-state emission spectra of $Re(CO)_3(2,2'\text{-biq})L_S^+$, L_S = pz; 4,4′-bipy, consisted of broad emission bands centered at 670 nm and exhibited insignificant changes with solvent, CH_3CN, MeOH, or CH_2Cl_2 containing 4% v/v CH_3OH, Figure 3b. The emission spectra of the two (2,2′-biq) complexes were nearly identical. A comparison of the spectra recorded with λ_{exc} = 350 or 400 nm and either one of the (2,2′-biq) complexes reveals two contributions to the luminescence, Figure 3b.

In addition to the intrinsic dependences of the emission spectra on solvent and/or λ_{exc}, a time-resolved study revealed also multiple contributions to the luminescence of the complexes.

Time-Resolved Luminescence. The decay of the luminescence was investigated in laser flash irradiations, λ_{exc} = 337 and 355 nm, of the complexes in deaerated solutions, Table 5. Since these experiments revealed no dependence of the luminescence lifetimes on λ_{exc}, they were calculated from the oscillographic traces recorded with 337 nm irradiations, i.e., where the signal-to-noise ratio was the best. A double exponential decay of the $Re(CO)_3(2,2'\text{-bipy})O_2C\text{-pz}$ emission in deaerated CH_3CN, $A_1\, e^{-t/\tau 1} + A_2\, e^{-t/\tau 2}$ with lifetimes τ_1 and τ_2, was slower than the single-exponential decay of the $Re(CO)_3(2,2'\text{-bipy})Br$ under similar conditions, Table 5.[4] The values of τ_1 and τ_2 exhibited little if any dependence on the monitoring wavelength between 550 and 700 nm.

The biexponential function gave also a good least-squares fitting of oscillographic traces for the luminescence decay of $Re(CO)_3(2,2'\text{-biq})L_S^+$, L_S = pz and 4,4′-bipy, Figure 4a, and the calculated lifetimes were longer

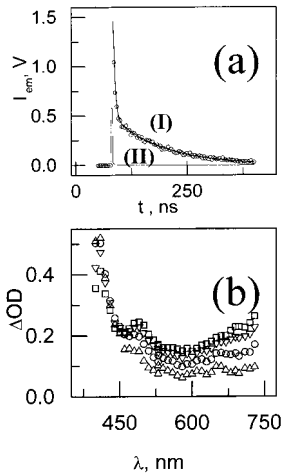

Figure 4. Trace (I) in (a) shows the biphasic decay of the luminescence when 5.0×10^{-4} M $Re(CO)_3(2,2'\text{-biq})pz^+$ in N_2-deaerated 4% v/v MeOH in CH_2Cl_2 is irradiated with 337 nm laser flashes. The 337 nm laser pulse used for the irradiation is shown in the trace (II). Early spectral changes, recorded with 355 nm flash irradiations of 5.0×10^{-4} M $Re(CO)_3(2,2'\text{-biq})pz^+$ in 4% v/v MeOH in CH_2Cl_2, are shown in (b). The delays from the laser irradiation are 2 ns, △; 4 ns, ○; 6 ns, ▽; 8 ns, □.

than those of the $Re(CO)_3(2,2'\text{-biq})Br$ luminescence, Table 5.[5] In addition, the long-lived component of the luminescence in $Re(CO)_3(2,2'\text{-biq})L_S^+$, L_S = pz, 4,4′-bipy, py, CH_3CN, and Br, Table 5, varied with L_S in a manner consistent with the relaxation of the Re(I) to (2,2′-biq) charge-transfer excited state.[5,6] The values of the luminescence lifetimes τ_1 and τ_2 calculated from traces recorded with λ_{exc} = 337 nm were, within experimental error, the same calculated from traces recorded with λ_{exc} = 355 nm. This result was also reflected in the agreement between the time-resolved emission and absorption observations communicated next.

Excited-State Absorption Spectra. Time-resolved absorption and emission spectroscopies provided complementary views of the excited-state kinetics. Flash photochemical irradiations, λ_{exc} = 351 or 355 nm, of $Re(CO)_3(2,2'\text{-biq})pz^+$ in deaerated CH_3CN containing 4% v/v MeOH induced short- and long-lived optical density changes. On a time scale of 10 ns after the laser irradiation, a partial decay of a 400 nm feature is simultaneous with the appearance of absorptions at λ_{ob} > 450 nm, Figure 4b. The decay of the latter occurs on a 0.3 μs time scale. By contrast to $Re(CO)_3(2,2'\text{-biq})pz^+$, the prompt spectra recorded in flash photochemical irradiations, λ_{exc}= 355 nm, of $Re(CO)_3(2,2'\text{-biq})4,4'\text{-bipy}^+$ in deaerated CH_3CN with 4% v/v MeOH exhibited a maximum at $\lambda_{max} \approx$ 370 nm and absorptions without a definite maximum at 650 > λ_{ob} > 450 nm. The optical density at λ_{ob} > 450 nm increased in relationship to the 370 nm maximum after the laser irradiation. However, the lifetime was too short, $\tau \leq$ 5 ns, to make a kinetic study.

In similar flash photolysis experiments with 1.0×10^{-4} M $Re(CO)_3(2,2'\text{-bipy})O_2C\text{-pz}$ in deaerated CH_3CN, the absorption band at 400 nm and absorptions at λ_{ob} > 450 nm were observed ~2 ns after the laser flash irradiation, Figure 5. This spectrum changed in the same time scale of the luminescence with a lifetime τ_1, Table 5. The demise of the transient spectrum occurred

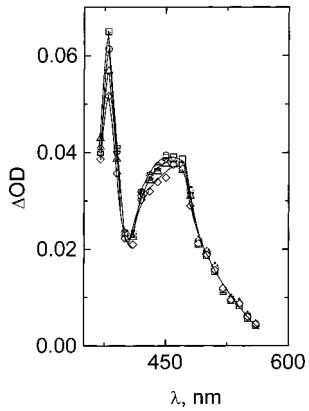

Figure 5. Early spectral changes recorded in 351 nm irradiations of 1.0×10^{-4} M $Re(CO)_3(2,2'\text{-bipy})O_2C\text{-pz}$ in CH_3CN. The delays from the laser irradiation are 2 ns, □; 4 ns, ○; 6 ns, △; 8 ns, ◊.

also with lifetimes similar to those calculated for the long-lived emission, Table 5.

Irradiations of the Re(I) complexes, $\lambda_{exc} = 350$ nm, with 10 to 20 laser flashes of less than 15 mJ/pulse, i.e., less than 10^{-5} einstein L^{-1} $flash^{-1}$ absorbed by the photolyte, did not cause permanent spectral changes; that is, no photolysis products appear to be formed in these photoprocesses.[31] Moreover, agreement between the lifetimes calculated via time-resolved absorption spectroscopy and those calculated via time-resolved emission spectroscopy indicates that the transient spectra can be assigned to the complexes in their excited states.

Pulse Radiolysis Experiments. The spectrum of one-electron-reduced species was recorded by pulse radiolysis. These experiments provided a basis for the assignment of species formed in redox reactions of the Re(I) complexes in MLCT excited states. Pulse radiolysis of 10^{-4} M $Re(CO)_3(2,2'\text{-bipy})O_2C\text{-pz}$ in N_2O-saturated methanol produced 6.7×10^{-6} or 3.3×10^{-6} M $^{\bullet}CH_2OH$ radicals in less than a microsecond. The $^{\bullet}CH_2OH$ radicals reacted on a longer time scale with $Re(CO)_3(2,2'\text{-bipy})O_2C\text{-pz}$ to produce the spectrum of $Re(CO)_3((2,2'\text{-bipy})^{\bullet})O_2C\text{-pz}^-$ via a reaction that was kinetically of pseudo-first-order. Assignment of the species was based on the resemblance of its absorption spectrum with a previously recorded spectrum of Re(I)-ligand radical species.[7,13] A rate constant $k = (5.8 \pm 0.3) \times 10^8$ M^{-1} s^{-1} was calculated as an average of rate constants from oscillographic traces recorded at λ_{ob} 300, 350, 480, and 540 nm. In N_2-saturated solutions of 10^{-4} M $Re(CO)_3(2,2'\text{-bipy})O_2C\text{-pz}$ in methanol, the optical densities at $\lambda_{ob} \leq 400$ nm were larger than those recorded in experiments with N_2O-saturated solutions. This spectrum decayed in an interval of 2 ms to the previous spectrum of $Re(CO)_3((2,2'\text{-bipy})^{\bullet})O_2C\text{-pz}^-$. Since ca. 3.4×10^{-6} M or 1.7×10^{-6} M e^-_{solv} are produced in these conditions together with an equimolar concentration of $^{\bullet}CH_2OH$ radicals, the additional absorptions must be associated with products of reactions between $Re(CO)_3(2,2'\text{-bipy})O_2C\text{-pz}$ and e^-_{solv}. Such absorptions could be assigned to either or both $Re^0(CO)_3(2,2'\text{-bipy})O_2C\text{-pz}^-$ and $Re^I(CO)_3(2,2'\text{-bipy})((O_2C\text{-pz})^{\bullet})^-$. The redox properties, Table 4, and the ligand-centered nature of the low-energy orbitals in these complexes give more support to the latter assignment. The slow spectral changes must be ascribed, therefore, to a transformation of one or both species into $Re(CO)_3((2,2'\text{-bipy})^{\bullet})O_2C\text{-pz}^-$.

Similar experimental observations were made in pulse radiolysis of 10^{-4} M $Re(CO)_3(2,2'\text{-biq})L_S$, L_S = 4,4′-bipy or pz, in MeOH. Species of Re(I) with coordinated $(2,2'\text{-biq})^{\bullet-}$ radicals were generated in N_2O-saturated solutions with rate constants $k = 9.8 \times 10^8$ M^{-1} s^{-1} for L_S = 4,4′-bipy and $k = 9.9 \times 10^8$ M^{-1} s^{-1} for L_S = pz. The spectrum generated in the reduction of $Re(CO)_3(2,2'\text{-biq})L_S$, L_S = 4,4′-bipy or pz, by $^{\bullet}CH_2OH$ radicals has features also found in the spectrum of $Re(CO)_3((2,2'\text{-biq})^{\bullet})Br^-$. The latter ligand-radical species was generated in pulse radiolysis of N_2O-saturated solutions containing 10^{-4} M $Re(CO)_3(2,2'\text{-biq})Br$ in MeOH. It must be noted that, in the reaction between $Re(CO)_3(2,2'\text{-biq})Br$ and $^{\bullet}CH_2OH$ radicals, the redox potentials of the reactants do not allow for the reduction of Re(I). The transient spectrum furnishes therefore a positive assignment of the Re(I)-ligand radical.

Excited-State Reduction. Reactions of the long-lived excited states of the Re(I) with 2,2′,2″-nitrilotriethanol, TEOA, were investigated by time-resolved absorption spectroscopy. The complexes were irradiated, $\lambda_{exc} = 351$ nm, in deaerated CH_3CN solutions containing ca. 10^{-4} M complex and 0.07−0.2 M TEOA. In less than 200 ns, the flash-generated spectra of the electronically excited complexes changed to those observed in pulse radiolysis. The latter spectra was therefore assigned to Re(I) species with coordinated $(2,2'\text{-bipy})^{\bullet-}$ or $(2,2'\text{-biq})^{\bullet-}$ radicals formed by an excited state redox reaction. On a longer time scale, the spectrum of the Re(I) ligand-radical species grew by a process, i.e., on a 100 μs time scale, that was initiated after the electron-transfer quenching had finished. The rate of the spectral growth increased with Re(I) concentration. Flash photolysis of deaerated solutions containing 0.2 M TEOA and 0.5×10^{-4} to 2.0×10^{-4} M concentrations of $Re(CO)_3(2,2'\text{-biq})4,4'\text{-bipy}^+$ or $Re(CO)_3(2,2'\text{-biq})pz^+$ showed that the process was kinetically of a pseudo-first-order. Nearly identical rate constants, $k = (2.4 \pm 0.2) \times 10^9$ M^{-1} s^{-1}, for the formation of the Re(I) ligand-radicals were calculated by following the optical changes at 480 nm. Since oxidation of TEOA in the electron-transfer quenching produces reducing radicals, i.e., $(HOCH_2CH_2)_2N(^{\bullet}CHCH_2OH)$,[34] and the growth was attributed to reactions between these radicals and Re(I) complexes.

(31) The use of $\lambda_{exc} \geq 337$ nm and low photonic energies minimized photodecomposition in these Re(I) complexes. However, photodecomposition was appreciable when large concentrations of photons were absorbed by the photolyte, i.e., > 20 mJ/pulse ≈ 10^{-5} einstein L^{-1} $flash^{-1}$, or when higher photonic energies, i.e., $\lambda_{exc} < 337$ nm, were used in flash photolysis.

(32) The reduction of the 2,2′-bipy has been previously investigated.[33] In our experiments, bleaching of the ligand absorptions associated with π to π^* electronic transitions suggests hydrogenation of the azine. While this process could be the most important one, additional products appear to be formed in the 360 nm continuous photolysis of the Re(I) complexes. This experimental observation suggests that there are several second-order terminations for the $Re(CO)_3((2,2'\text{-biq})^{\bullet})L_S$ species.

(33) (a) Simic, M.; Ebert, M. *Int. J. Radiat. Phys. Chem.* **1971**, *3*, 259. (b) Krishnan, C. V.; Creutz, C.; Schwarz, H. A.; Sutin, N. *J. Am. Chem. Soc.* **1983**, *105*, 5617. (c) Erkhard, H.; Jaenicke, W. *Electroanal. Chem.* **1975**, *65*, 675.

(34) See pp 1361, 1362 in: Kirch, M.; Lehn, J. M.; Sauvage, J. P. *Helv. Chim. Acta* **1979**, *62*, 1345.

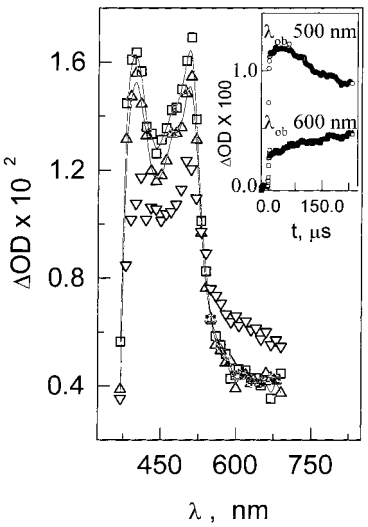

Figure 6. Transient spectra of species generated in the 351 nm irradiation of deaerated 1.0×10^{-4} M $Re(CO)_3(2,2'\text{-bipy})O_2C\text{-pz}$ and 0.73 M TEOA in CH_3CN. Delays of 200 ns, △, 40 μs, □, and 200 μs, ▽, after the laser flash were used in the experiments. The inset shows two traces for the decay of $Re(CO)_3((2,2'\text{bipy})^{\bullet})O_2C\text{-pz}^-$, $\lambda_{ob} = 500$ nm, and formation of $Re(CO)_3(2,2'\text{-bipyH}_2)O_2C\text{-pz}$, $\lambda_{ob} = 600$ nm at $t > 40$ ns.

In these experiments, the demise of the Re(I) ligand-radical species was observed on a time scale of 10^2 ms. Acceptable straight lines fitted to plots $1/\Delta OD$ vs t proved that those processes leading to the disappearance of the Re(I) ligand-radical species were kinetically of second order. The values for the ratio of the rate constant to the extinction coefficient, $k/\epsilon = 6.5 \times 10^3$ cm s^{-1} for L_S = 4,4′-bipy and $k/\epsilon = 2.4 \times 10^4$ cm s^{-1} for L_S = pz, were calculated by such least-squares fitting of data collected at λ_{ob} 480 nm. The second-order reactions of $Re(CO)_3((2,2'\text{-biq})^{\bullet})L_S$ can be attributed to their disproportionation into the parent complex and $Re(CO)_3((2,2'\text{-biq})H_2)L_S$, i.e., a species where a double bond of the (2,2′-biq) ligand has been hydrogenated.[13,32,33]

A transient spectrum recorded several microseconds after the excited state of $Re(CO)_3(2,2'\text{-bipy})O_2C\text{-pz}$ reacted with 0.7 M TEOA in CH_3CN is shown in Figure 6. This spectrum is similar to one recorded after the reduction of the Re(I) complex by $^{\bullet}CH_2OH$ radicals in pulse radiolysis. Therefore, the spectral changes observed several microseconds after the quenching has finished are in accordance with the reduction of coordinated 2,2′-bipy to give $Re(CO)_3((2,2'\text{-bipy})^{\bullet})O_2C\text{-pz}^-$. By contrast to the (2,2′-biq) complexes, little if any $Re(CO)_3(2,2'\text{-bipy})^{\bullet})O_2C\text{-pz}^-$ was produced by reactions of $Re(CO)_3(2,2'\text{-bipy})O_2C\text{-pz}$ with radicals from the oxidation of TEOA. However, the spectral changes on a 200 μs time scale corresponded to the formation of a Re(I) complex with a hydrogenated 2,2′-bipy ligand, e.g., 2,2′-bipyH_2, Figure 6.[13,32,33] The process is too fast to be the disproportionation of Re(I) ligand-radicals, i.e., one observed on a 10^2 ms time scale with $Re(CO)_3((2,2'\text{-biq})^{\bullet})L_S$ species. These experimental observations suggest that TEOA radicals reduced a fraction of the $Re(CO)_3((2,2'\text{-bipy})^{\bullet})O_2C\text{-pz}^-$ that were formed during the quenching of the excited state. The remaining fraction of $Re(CO)_3((2,2'\text{-bipy})^{\bullet})O_2C\text{-pz}^-$ radicals decayed on a 10^2 ms time scale by a process with second-order kinetics. A linear least-squares fitting of plots $1/\Delta OD$ vs t gave values of $k/\epsilon \approx 4.7 \times 10^5$ cm s^{-1} at λ_{ob} 510 nm.

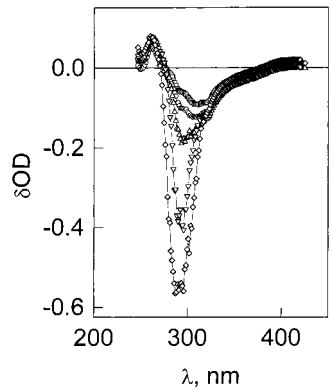

Figure 7. Typical difference spectrum of $Re(CO)_3(2,2'\text{-bipy})O_2C\text{-pz}$ in the presence of various $CuCl_2$ concentrations. Each difference spectrum was calculated by subtracting from the spectrum of a solution containing 1.0×10^{-4} M Re(I) complex and a given concentration of $CuCl_2$ the spectra of two solutions. One solution contained only $CuCl_2$ in the same concentration of the former solution, and the other solution contained only 1.0×10^{-4} M Re(I) complex. The $CuCl_2$ concentrations in 4% v/v MeOH in CH_2Cl_2 are 1.0×10^{-3} M, □, 2.0×10^{-3} M, ○, 3.0×10^{-3} M, △, 4.0×10^{-3} M, ▽, 5.0×10^{-3} M, ◇.

Ground State Adducts. Changes in the UV−vis absorption spectrum revealed the formation of adducts between the Re(I) complexes and $CuCl_2$, eq 7

$$Re(CO)_3L_AL_S^{\,z} + CuCl_2 \rightleftarrows Re(CO)_3L_A(Cl_2Cu\text{-}L_S)^z, \text{ where } z = + \text{ or } 0 \quad (7)$$

Indeed, the respective spectrum of $CuCl_2$ and $Re(CO)_3L_AL_S^z$, $z = 0$ or +, did not add to the spectrum of a solution containing both species. Typical difference spectra recorded with solutions containing 1.0×10^{-4} M $Re(CO)_3(2,2'\text{-bipy})O_2C\text{-pz}$ and various concentrations of $CuCl_2$ between 1.0×10^{-3} and 5.0×10^{-3} M are shown in Figure 7. Such difference spectra were calculated by subtracting the spectra of two solutions containing respectively one of the Re(I) complexes and $CuCl_2$ from the spectrum of a solution having these species together and in the same concentrations of the two previous solutions. In Figure 7, the absorption band that is primarily affected by $CuCl_2$ corresponds to an intraligand transition of the pz-CO_2^- ligand at $\lambda_{ob} \approx 290$ nm. By contrast, there is little change in the spectral region corresponding to a Re(I) to 2,2′-bipy charge-transfer transition, i.e., $\lambda_{ob} > 350$ nm. Since similar modifications in the spectrum of the Re(I) complexes were observed when $CuCl_2$ was replaced by triflic acid, the ligand L_S must have sufficient basic character to undergo protonation or coordination to $CuCl_2$. In this regard, the modifications in the spectrum probably reflect electronic changes in the spectator ligand.

The equation $\delta OD_{\lambda_{ob}}^{-1} = (C \times \Delta\epsilon)^{-1} + (C \times \Delta\epsilon \times K)^{-1} \times [CuCl_2]^{-1}$ gives the difference, $\delta OD_{\lambda_{ob}}$, between the optical densities of two solutions with the same total concentration, C, of Re(I) complex and different concentrations of $CuCl_2$, i.e., one with a $[CuCl_2] \neq 0$ concentra-

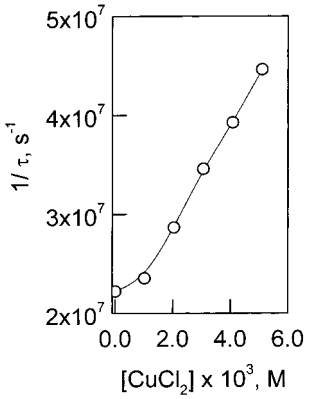

Figure 8. Stern−Volmer plot for the $CuCl_2$ quenching of the slow component of the $Re(CO)_3(2,2'\text{-bipy})O_2C\text{-pz}$ emission. Solutions in 4% v/v MeOH in CH_2Cl_2 were deaerated with N_2.

tion and the other with no $CuCl_2$. K is the equilibrium constant of eq 7, and $\Delta\epsilon$ is the difference between the extinction coefficients of the Re(I) adduct and the Re(I) complex at a wavelength λ_{ob}. Several plots of $\delta OD_{\lambda ob}{}^{-1}$ vs $[CuCl_2]^{-1}$ were made for each complex by measuring the optical density changes at various wavelengths. Rough values of K were calculated from these linear plots, i.e., $K = (2.8 \pm 0.3) \times 10^2\ M^{-1}$ for the adduct of $Re(CO)_3(2,2'\text{-bipy})O_2C\text{-pz}$ and $K \leq (1.3 \pm 0.3) \times 10^2\ M^{-1}$ for the adducts of $Re(CO)_3(2,2'\text{-biq})4,4'\text{-bipy}^+$ and $Re(CO)_3(2,2'\text{-biq})pz^+$.

The luminescence of $Re(CO)_3(2,2'\text{-bipy})O_2C\text{-pz}$ and $Re(CO)_3(2,2'\text{-biq})L_S{}^+$, L_S = pz or 4,4′-bipy, was also quenched in the range of $CuCl_2$ concentrations indicated above. A progressive quenching of the emission by $CuCl_2$ causes also some small changes in the band shape. A displacement of the maximum by 5 nm toward longer wavelengths and a broadening of the band, i.e., a 6 nm change in width, were observed in the range of $CuCl_2$ concentrations indicated above. In 337 nm flash fluorescence experiments with 1×10^{-4} M $Re(CO)_3(2,2'\text{-biq})4,4'\text{-bipy}^+$ and $Re(CO)_3(2,2'\text{-biq})pz^+$, quenching of the emissions by 1×10^{-5} to 5.0×10^{-3} M $CuCl_2$ has no effect on the rate of the fast component. Solutions of $Re(CO)_3(2,2'\text{-bipy})O_2C\text{-pz}$ in CH_2Cl_2 containing also 1×10^{-5} to 5.0×10^{-3} M $CuCl_2$ were used for the investigation of the emission kinetics at $\lambda_{ob} = 650$ nm. Flash fluorescence measurement, i.e., $\lambda_{exc} = 337$ nm, showed that the rate of the fast component of the emission increased with $CuCl_2$. The rate of the emission increased until only the emission's slowest component was observed, i.e., when Cu(II) concentrations were larger than 10^{-3} M. Above this concentration, a single exponential, $e^{-t/\tau}$, was fitted to oscillographic traces for the calculation of emission lifetimes. Although the reciprocal of the lifetime increased with $CuCl_2$ concentration, plots of τ^{-1} vs $[CuCl_2]$ deviated from a straight line. Such deviations were more pronounced in the plot made for the quenching of the $Re(CO)_3(2,2'\text{-bipy})O_2C\text{-pz}$ luminescence, Figure 8.

The quenching of the luminescence was also investigated by flash photolysis under the same conditions indicated above. Products from an electron-transfer quenching were not observed in these experiments.

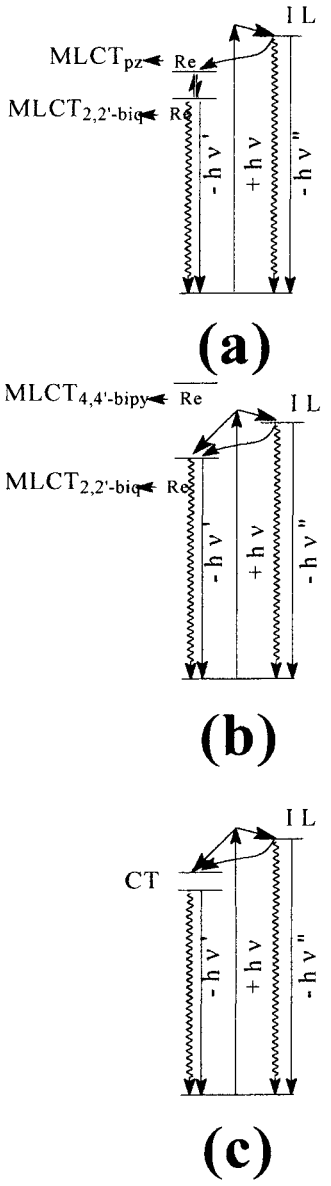

Figure 9. Excited state energy diagrams and relevant relaxation processes in (a) $Re(CO)_3(2,2'\text{-biq})pz^+$, (b) $Re(CO)_3(2,2'\text{-biq})(4,4'\text{-bipy})^+$, and (c) $Re(CO)_3(2,2'\text{-bipy})O_2C\text{-pz}$. The diagrams show the result of the irradiation near 350 nm, and the ordinate, energy, does not provide a quantitative measure of the separation between electronic levels.

Discussion

Notwithstanding structural similarities of $Re(CO)_3(2,2'\text{-biq})4,4'\text{-bipy}^+$, $Re(CO)_3(2,2'\text{-biq})pz^+$, and $Re(CO)_3(2,2'\text{-bipy})O_2C\text{-pz}$ with other Re(I) complexes in the literature reports, the compounds in this study yielded new insights on the their excited-state properties. Such properties will be discussed next in terms of the energy and electron-transfer reactions and photophysical processes.

IL and MLCT Excited States. Photophysical processes relevant to the discussion of the time-resolved spectroscopies of $Re(CO)_3(2,2'\text{-biq})4,4'\text{-bipy}^+$, $Re(CO)_3(2,2'\text{-biq})pz^+$, and $Re(CO)_3(2,2'\text{-bipy})O_2C\text{-pz}$ are shown in Figure 9. The absorption spectra of the complexes in Figure 2 have features that in related Re(I) complexes have been associated with intraligand and low-

energy Re(I) to L_A charge-transfer transitions.[2−7] Irradiations of $Re(CO)_3(2,2'\text{-biq})L_S^+$ between 337 and 355 nm are within a band, Figure 2, that is the envelop for a Re(I) to (2,2′-biq) charge-transfer transition and an intraligand transition centered in the (2,2′-biq) ligand. Also, the emission spectra of the $Re(CO)_3(2,2'\text{-biq})L_S^+$, L_S = 4,4′-bipy or pz, in Figure 3 show some of the features seen early in the spectra of $Re(CO)_3(2,2'\text{-biq})$Br and related complexes.[5,7] The dependence of the emission spectrum on excitation wavelength, Figure 3, indicates that two emissive states are populated with irradiations between 337 and 400 nm. This observation is corroborated by the biexponential kinetics of the luminescence and the results of time-resolved absorption spectroscopy, Table 5 and Figure 4. In these regards, the biexponential rate of the $Re(CO)_3(2,2'\text{-biq})L_S^+$, L_S = 4,4′-bipy or pz, luminescence can be associated with the decays of a long-lived and a short-lived excited state, Table 5. It was established in a previous work[5] that a short-lived IL excited state of the (2,2′-biq) ligand is placed between 15 and 20 kJ above the $MLCT_{(2,2'-biq)\leftarrow Re}$ charge-transfer state. Therefore, the fast component of the luminescence with a lifetime τ_1 can be assigned to the IL excited state. This assignment is in accordance with the lack of absorption features at λ_{ob} >390 nm in the absorption spectrum of this excited state, i.e., the prompt transient spectrum recorded in 355 nm flash photolysis of $Re(CO)_3(2,2'\text{-biq})pz^+$, Figure 4b. The growth of the optical density at $\lambda_{ob} \geq 390$ nm, characteristic in most of these compounds of a $MLCT_{(2,2'-biq)\leftarrow Re}$ excited state,[5] and the fast component, $e^{-t/\tau 1}$, in decay of the luminescence, Table 5 and Figure 4, take place on the same time scale. This observation shows that no MLCT state is formed by the 355 nm laser photolysis, and the irradiation of $Re(CO)_3(2,2'\text{-biq})pz^+$ at such a wavelength must selectively populates the IL excited state. It is the decay of the IL state that brings some population to the MLCT, as shown in Figure 9a.

The slow component of the emission, $e^{-t/\tau 2}$, and the long-lived transient observed with $\lambda_{ob} \geq 390$ nm in flash photolysis can be ascribed to several charge-transfer excited states, e.g., $MLCT_{LS\leftarrow Re}$, $MLCT_{LA\leftarrow Re}$, $CT_{LA\leftarrow LS}$, and/or $CT_{LS\leftarrow LA}$. Reduction potentials for $pz/pz^{\bullet -}$ and Re(II)/Re(I) couples, Table 4, suggest that $MLCT_{pz\leftarrow Re}$ and $MLCT_{(2,2'-biq)\leftarrow Re}$ excited states in $Re(CO)_3(2,2'\text{-biq})pz^+$ could be close in energy. If they are as close as indicated by the potentials, the slow decay of the emission and the growth of the MLCT spectrum must occur when the two excited states, $MLCT_{pz\leftarrow Re}$ and $MLCT_{(2,2'-biq)\leftarrow Re}$, are in equilibrium, Figure 9a. A literature report has shown that conversions between charge-transfer states by means of an intraligand electron transfer can be very fast.[4,35,36] It is possible, therefore, that the $MLCT_{pz\leftarrow Re}$ and the $MLCT_{(2,2'-biq)\leftarrow Re}$ achieve equilibration in a time shorter than τ_2 or it would have been observed in our time-resolved emission and/or absorption experiments. In addition, at least one of these excited sates must decay with a lifetime close to $\tau_2 \approx 10^2$ ns to account for the long-lived exponential decay, Table 5 and Figure 4.

By contrast to $Re(CO)_3(2,2'\text{-biq})pz^+$, irradiations of $Re(CO)_3(2,2'\text{-biq})4,4'\text{-bipy}^+$ between 337 or 355 nm in flash photolysis and flash fluorescence experiments did not specifically populate the IL excited state. The spectrum of the excited state and the kinetics of the luminescence showed a simultaneous population of the IL and MLCT excited states, Figure 9b. The potentials for the 4,4′-bipy/$4,4'\text{-bipy}^{\bullet -}$ and (2,2′-biq)/$(2,2'\text{-biq})^{\bullet -}$ couples indicate that the $MLCT_{4,4'-bipy\leftarrow Re}$ excited state is probably too high in energy. It will not be populated with the range of photonic energies, $E_{h\nu} < 360$ kJ/mol, used in this work, and it is shown, therefore, above the photonic energy in Figure 9b. Transients with a lifetime τ_2 in emission and optical absorption experiments must be associated with the decay of a Re(I) to (2,2′-biq) charge-transfer excited states.[6,4]

The photobehavior of $Re(CO)_3(2,2'\text{-bipy})O_2C$-pz departs to some degree from the one observed with the (2,2′-biq) complexes. Indeed, one contribution to the emission is very solvent dependent and too low in photonic energy to originate from intraligand states of the 2,2′-bipy or pz-CO_2^- ligands, Figure 3. This solvent-dependent contribution to the steady-state emission must be related to charge-transfer excited states. The hypsochromic shift of the emission with increasing excitation wavelength, Figure 3, suggests that the MLCT excited state is considerably distorted with respect to the ground state. In addition to the optical absorptions of the MLCT, the transient spectrum in Figure 4b has a feature with $\lambda_{max} \leq 380$ nm that can be assigned to an IL excited state. Conversion of this IL state into the MLCT on a time scale $t \leq 20$ ns results in a slight increase of the absorptions with $\lambda_{ob} \geq 390$ nm, Figure 5. In terms of the time scales, it is possible to associate such spectral changes with the $e^{-t/\tau 1}$ component of the luminescence decay, Table 5. The process resembles therefore one observed in the $Re(CO)_3(2,2'\text{-biq})4,4'\text{-bipy}^+$ photolysis, Figure 9b,c. The long-lived transient spectrum with a lifetime τ_2 and an absorption band centered at 450 nm in the transient spectrum may correspond to MLCT excited states. Redox potentials in Table 4 suggest that the optical transients are likely related to a mixture of excited states, e.g., $MLCT_{(2,2'-bipy)\leftarrow Re}$ and $MLCT_{(pzCO_2)\leftarrow Re}$, denoted as CT in Figure 9c.

Reductive Quenching. The electron-transfer reactions of the excited Re(I) complexes with TEOA did not discriminate between the two different types of excited states, i.e., MLCT. In the following discussion these states will be identified as $^*Re(CO)_3\ L_AL_S^z$, where L_A = 2,2′-bipy, L_S = pz-CO_2^-, z = 0 or L_A= (2,2′-biq), L_S = 4,4′-bipy, pz, z = +. Previous work[5,7,13] and pulse radiochemical experiments indicated that products of the TEOA reactions with excited states, eq 8, are Re(I) complexes with a coordinated $(2,2'\text{-biq})^{\bullet -}$ or $(2,2'\text{-bipy})^{\bullet -}$ ligand-radical.

$$^*Re(CO)_3L_AL_S^{\ z} + TEOA \rightarrow Re(CO)_3(L_A^{\bullet})L_S^{(z-1)} + TEOA^+ \quad (8)$$

A reaction of $TEOA^+$ with TEOA produces radicals capable of reducing $Re(CO)_3(2,2'\text{-biq})L_S^+$, L_S = 4,4′-bipy,

(35) Parallel paths for the degradation of electronic energy have also been observed with Re(I) complexes having IL and charge-separated states lying below the MLCT.[4,36] No spectroscopic evidence in this work gave indication that ligand to ligand charge-separated states participated in the photophysical processes of $Re(CO)_3(2,2'\text{-biq})4,4'\text{-bipy}^+$ and $Re(CO)_3(2,2'\text{-biq})pz^+$.

(36) Liard, D. J.; Vlceck, A., Jr. *Inorg. Chem.* **2000**, *39*, 485.

pz, complexes and to a minor extent $Re(CO)_3(2,2'\text{-bipy})O_2C\text{-pz}$, eq 9.

$$TEOA + TEOA^+ \rightarrow (HOCH_2CH_2)_2N{-}\dot{C}H{-}CH_2OH + HTEOA^+ \quad (9)$$

In flash photolysis, the reduction of the Re(I) complexes by the radicals was observed as a growth of the $Re(CO)_3(HL_A^{\bullet})L_S^{z}$ spectrum on a time scale of 200 μs, eq 10.

$$Re(CO)_3(L_A)L_S^{z} + (HOCH_2CH_2)_2N{-}\dot{C}H{-}CH_2OH \rightarrow Re(CO)_3(L_A^{\bullet})L_S^{z-1} + (HOCH_2CH_2)_2N^+{=}CHCH_2OH \quad (10)$$

On a similar time scale, $Re(CO)_3(2,2'\text{-bipyH}_2)O_2C\text{-pz}$ does not react according to eq 10, and spectral transformations in Figure 5 correspond to a partial decay of the $Re(CO)_3((2,2'\text{bipy})^{\bullet})O_2C\text{-pz}^-$ spectrum and the formation of $Re(CO)_3(2,2'\text{-bipyH}_2)O_2C\text{-pz}$, a common product in the reduction of pyrazine radicals. Equation 11 provides, therefore, a good description of the experimental observations.

$$Re(CO)_3(2,2'\text{-bipy}^{\bullet})O_2C\text{-pz}^- + 2H^+ + (HOCH_2CH_2)_2N{-}\dot{C}H{-}CH_2OH \rightarrow Re(CO)_3(2,2'\text{-bipyH2})O_2C\text{-pz} + (HOCH_2CH_2)N^+{=}CHCH_2OH \quad (11)$$

The fraction of $Re(CO)_3((2,2'\text{bipy})^{\bullet})O_2C\text{-pz}^-$ not consumed via eq 11 and $Re(CO)_3((2,2'\text{-biq})^{\bullet})L_S$, L_S = pz, 4,4′-bipy, radicals survive times $t > 10^2$ ms in solutions where their concentrations are between 10^{-5} and 10^{-6} M. Literature reports suggest that the termination reactions of these radicals are disproportionation processes, eq 12.

$$2Re(CO)_3(L_A^{\bullet})L_S^{z-1} + 2H^+ \rightarrow Re(CO)_3(H_2L_A)L_S^{z} + Re(CO)_3L_AL_S^{z} \quad (12)$$

Since TEOA radicals reduce $Re(CO)_3((2,2'\text{bipy})^{\bullet})O_2C\text{-pz}^-$ via eq 11, but are unable to react in the same manner with $Re(CO)_3((2,2'\text{-biq})^{\bullet})L_S$, the former must be a better oxidant than the latter species. No reduction of the spectator ligand L_S or ligand-to-ligand electron transfer, i.e., processes similar to those undergone by $Re(CO)_3$-(1,10-phenanthroline)4-nitrobenzoato,[6] were observed with these complexes. Pulse radiolysis shows that a reductant as strong as e^-_{solv} is able to generate small concentrations of Re complexes reduced either at the metal center or at ligands other than (2,2′-biq) and 2,2′-bipy.

Adducts and Energy Transfer. Results from steady-state and time-resolved experiments indicate the effect of $CuCl_2$ on the luminescence of the Re(I) complexes must be associated with more than one quenching process. These processes involve the excited complexes $*Re(CO)_3\ L_AL_S^{z}$ and the excited adducts $*Re(CO)_3\ L_A(CuCl_2\text{-}L_S)^{z}$, previously described in eq 7. Although the IL and MLCT excited states are simultaneously produced by the 350 or 337 nm laser excitations, they decay with different rates; that is, they were observed on very different time scales. In this regard, the experimental observations can be described by eqs 13−20.

$$Re(CO)_3L_AL_S^{z} + h\nu \rightarrow *Re(CO)_3L_AL_S^{z} \quad (13)$$

$$*Re(CO)_3L_AL_S^{z} \rightarrow Re(CO)_3L_AL_S^{z} + h\nu' \quad (14)$$

$$*Re(CO)_3L_AL_S^{z} \rightarrow Re(CO)_3L_AL_S^{z} \quad (15)$$

$$Re(CO)_3L_A(Cl_2Cu\text{-}L_S)^{z} + h\nu \rightarrow *Re(CO)_3L_A(Cl_2Cu\text{-}L_S)^{z} \quad (16)$$

$$*Re(CO)_3L_A(Cl_2Cu\text{-}L_S)^{z} \rightarrow Re(CO)_3L_A(Cl_2Cu\text{-}L_S)^{z} + h\nu' \quad (17)$$

$$*Re(CO)_3L_A(Cl_2Cu\text{-}L_S)^{z} \rightarrow Re(CO)_3L_A(Cl_2Cu\text{-}L_S)^{z} \quad (18)$$

$$*Re(CO)_3L_AL_S^{z} + CuCl_2 \rightarrow Re(CO)_3L_AL_S^{z} + {}^+CuCl_2 \quad (19)$$

$$*Re(CO)_3L_A(Cl_2Cu\text{-}L_S)^{z} + CuCl_2 \rightarrow Re(CO)_3L_A(Cl_2Cu\text{-}L_S)^{z} + *CuCl_2 \quad (20)$$

In the mechanism, eqs 14, 15, 17, and 18 are the radiative and radiationless relaxations of the electronically excited species respectively prepared in eqs 13 and 16. The eqs 19 and 20 have to be included in order to account for the quenching of the fast and slow components of the emission. Quenching of the fast component, fc, of the $Re(CO)_3(2,2'\text{-bipy})O_2C\text{-pz}$ emission by $CuCl_2$ occurs at concentrations where no adduct is formed. A quenching rate constant $k_{14}^{fc} \approx 8 \times 10^{10}$ M^{-1} s^{-1} was calculated for the fast component of the emission. Because of the short time scale of the quenching events, the rate constant can be associated with a bimolecular reaction between $CuCl_2$ and the short-lived IL excited state, eq 19. Deviations from linearity in plots $1/\tau_2$ vs $[CuCl_2]$ for the quenching of the slow component, sc, of the luminescence occur in a range of $CuCl_2$ concentrations, $[CuCl_2] > 10^{-4}$ M, where the formation of adduct is appreciable. However, the formation of, adducts, excited adducts, eq 16, and the adducts radiationless relaxation, eq 18, do not account by themselves for the functional dependence of $1/\tau_2$ on $[CuCl_2]$. To rationalize the such afunctional dependence, e.g., in Figure 7, the luminescence of the adducts, eq 17, and the quenching of such a luminescence, eq 20, must be incorporated in the mechanism. A solution of the rate equations for $*Re(CO)_3L_AL_S^{z}$ and $*Re(CO)_3L_A(CuCl_2\text{-}L_S)^{z}$ on the time scale of the emission's slow component gives the time dependence of the light intensity, eq 21.

$$I_{em}^{sc} = k_9^{sc}[*Re(CO)_3L_1L_S^{z}] + k_{12}^{sc}[*Re(CO)_3L_1(CuCl_2\text{-}L_S)^{z}]$$

where $[*Re(CO)_3L_1L_S^{z}] \approx [*Re(CO)_3L_1L_S^{z}]_{t=0}\ e^{-(k_{14}^{sc}+k_{15}^{sc}+k_{19}^{sc}[CuCl_2])t}$

and $[*Re(CO)_3L_1(CuCl_2\text{-}L_S)^{z}] \approx [*Re(CO)_3L_1(CuCl_2\text{-}L_S)^{z}]_{t=0}\ e^{-(k_{17}^{sc}+k_{18}^{sc}+k_{20}^{sc}[CuCl_2])t}$ (21)

In eq 21, $[*Re(CO)_3L_AL_S^{z}]_{t=0}$ and $[*Re(CO)_3L_A(CuCl_2\text{-}L_S)^{z}]_{t=0}$ are the flash-generated instantaneous concentrations of each species. If $*Re(CO)_3L_A(CuCl_2\text{-}L_S)^{z}$ decays only via raditionless relaxation processes, i.e., k_{17}^{sc} =

0, the second term of eq 21 vanishes for all $CuCl_2$ concentrations. In this particular case, it is, $1/\tau = (k_{14}^{sc} + k_{15}^{sc} + k_{19}^{sc} \times [CuCl_2])$, i.e., $1/\tau$ is linearly dependent on the $CuCl_2$ concentration. To observe departures from linearity in plots $1/\tau$ vs $[CuCl_2]$, the MLCT excited states in the Re(I) complex and in its adduct must have different lifetimes, i.e., $k_{14}^{sc} + k_{15}^{sc} \neq k_{17}^{sc} + k_{18}^{sc}$. In addition, it is the displacement of the equilibrium, eq 7, with $CuCl_2$ concentration that shifts the weight of the first to the second term in eq 16. If these two conditions are not fulfilled, deviations from linearity will not be observed. A least-squares polynomial expansion of eq 21 and lifetimes reported in Table 5 give a good fitting of the data in Figure 7 with $k_{19}^{sc} \approx 4 \times 10^9\ M^{-1}\ s^{-1}$.

Conclusions

The experimental observations in this work illustrate that the spectator ligand, L_S, can be conveniently insulated from ground and excited state electron transfers of the chromophore, $-Re(CO)_3L_A$. In this role, the spectator ligand L_S only modifies the properties of the chromophore instead of chemically competing with it. To make such charge transfer to L_S effective or to create charge-separated states, L_S ligands must be better oxidants, e.g., 4-nitrobenzoate or porphyrins, or possess excited states positioned at considerably lower energies than the chromophore's MLCT.

Acknowledgment. G.F. and E.W. acknowledge support from the Office of Basic Energy Sciences of the U.S. department of Energy. This is contribution No. NDRL-4191 from the Notre Dame Radiation Laboratory. E.W. also thanks the Fulbright Foundation for additional support. S.A.M. and J.G. respectively acknowledge support from the FONDECYT projects No. 1980374 and No. 2950074-95. G.F. wishes to acknowledge support from NSF, Grant No. INT97-26738.

Supporting Information Available: Crystal structure listings of crystal and refinement data, bond distances and angles, and thermal parameters. This material is available free of charge via the Internet at http://pubs.acs.org.

OM000784P